Project:

HyperOLED

(Grant Agreement number 732013)

"Development of high-performance, hyperfluorescence OLEDs for use in display applications and solid state lighting"

Funding Scheme: Research and Innovation Action

Call: ICT-02-2016 "Thin, Organic and Large Area Electronics"

Date of the latest version of ANNEX I: 12/10/2016

D4.2 Revised emitter characterisation set-up

Project Coordinator (PC):	Dr. Christof PFLUMM Merck Kommandit Gesellschaft auf Aktien
Project website address:	www.hyperoled.eu
Lead Partner for Deliverable:	Fraunhofer-IOF
Report Issue Date:	10/01/2018

Document History (Revisions – Amendments)	
Version and date	**Changes**
1.0 – 30/11/2017	initial version
1.1 – 19/12/2017	All data introduced, preliminary version
2.0 – 10/01/2018	Final version

Dissemination Level		
PU	Public	**X**
PP	Restricted to other program participants (including the EC Services)	
RE	Restricted to a group specified by the consortium (including the EC Services)	
CO	Confidential, only for members of the consortium (including the EC)	

The H2020 HyperOLED project is a three-year EC funded project entitled “Development of high-performance, hyperfluorescence OLEDs for use in display applications and solid state lighting”. The project will run from January 2017 to December 2019.

The overall goal of the HyperOLED project is to develop materials and matching device architectures for high performance, hyperfluorescence organic light emitting diodes (OLEDs) for use in display applications and solid state lighting. The innovative OLEDs will be realised by combining thermally activated delayed fluorescence (TADF) molecular hosts with novel shielded fluorescence emitters, targeting saturated blue emission of very high efficiency, especially at high-brightness levels.

Further efficiency gains will be achieved through molecular alignment to enhance light outcoupling from the hyperfluorescence OLEDs. Using shielded emitters will enable simpler device structures to be used, keeping drive voltages low to be compatible with low voltage CMOS backplane electronics. This will enable demonstration of the concept’s feasibility for high-brightness, full-colour OLED microdisplays as one application example.

To develop the hyperfluorescence OLEDs, the following scientific and technical objectives will be targeted:

- Objective 1: Develop shielded emitters
- Objective 2: Develop TADF hosts
- Objective 3: Photo-physically characterise the shielded emitters and TADF hosts
- Objective 4: Anisotropic molecular orientation for enhanced performance
- Objective 5: Design and test prototype hyperfluorescence OLEDs
- Objective 6: Fabricate and evaluate demonstration hyperfluorescence microdisplays

To show the project’s overall goal has been achieved, multiple blue and white stack unit prototypes (2 x 2 mm² on 30x30mm glass substrates with ITO) will be integrated into a high-brightness microdisplay demonstrator (based on MICROOLED’s 0.38’’ WVGA CMOS backplane) and tested that demonstrate significant improvements in functionality, performance, manufacturability and reliability.

Table of Contents

1 Introduction 4
1.1 Aim of emitter orientation analysis 4
1.2 Current approaches for orientation analysis 4
1.3 Theoretical description 4
1.4 Limitations and target 5
2 Experimental Set-up 6
2.1 Principle of operation 6
2.2 Sample design 6
2.3 Experimental set-up design 9
2.4 Final System 11
2.5 Preliminary experimental results 11
3 Summary and Conclusions 14
3.1 Summary 14
3.2 Outlook 14

1 Introduction

1.1 Aim of emitter orientation analysis

Emitter orientation is one parameter for optimizing the external OLED efficiency and brightness, because different emitter orientations suffer from different losses and feature different preferred emission directions. Therefore, analysing the orientation distribution of any emitting molecular ensemble is a prerequisite for an optimization of the emitting molecules as well as their hosts.

The impact of molecular orientation increases in the context of hyperfluorescence. The fluorophore's orientation (as acceptor of the energy transfer) remains target of optimization in order to achieve optimum outcoupling efficiency from the high index organic thin film layers, similarly to any standard device optimization. Additionally, the donor – fluorophore energy transfer, which is considered to be of Förster type,[1] depends on the relative orientation of the donor's emissive and the fluorophore's absorptive transition dipole moments.

So the detailed knowledge of molecular orientation distribution(s) is required in order to achieve a correct model of the hyperfluorescence energy transfer as well as an optimized out coupling based on the fluorophore's orientation. The present task introduces a set-up that will enable an improved characterization of the molecular ensemble's orientation distribution.

1.2 Current approaches for orientation analysis

Due to its impact on device efficiency, the experimental quantification of emitter orientation has been discussed frequently:

Initially, the orientation of conjugated polymers has been discussed with regard to its emission patterns[2,3] and lifetimes. Later on, such approaches were complemented by analysing the electroluminescence emission pattern of special devices[4,5] to enable for a quantitative orientation measurement. The emission pattern of supported thin emitting films can be utilized as well when pumping the emitters optically.[6]

All methods, independent of the electrical or optical pumping scheme, rely on the quantitative analysis of both the TE (s) and the TM (p) polarized emission patterns vs. the angle of emission. The ratio between the intensities observed for the two polarizations indicates the orientation of the emitting ensemble.

As an alternative approach one can consider the excited state's emission lifetime that depends on the orientation of the emitting transition dipole moment, too. One can observe strong effects especially near a metal surface. This is because perpendicularly oriented emitters suffer from a strong coupling to the surface plasmon polariton (SPP) at the metal surface, thus increasing the rate of emission and decreasing the emission lifetime. As the OLED contains a metal cathode, variations of the excited state lifetime vs. emitter cathode separation can be used for decay time based 3[,7,8] experimental determination of the orientation.

1.3 Theoretical description

With regard to a short description of such analyses, we utilize the approach published elsewhere5. The stationary emission, i.e. the pattern observed for any continuously pumped dipole source is described by

$$I^{stat}(\theta,\varphi) = \sin^2(\varphi)\left(I_{||,TE}(\theta) + I_{||,TM}(\theta)\right) + \cos^2(\varphi) * I_{\perp,TM}(\theta) \quad (1)$$

for the observation angle θ and the angle φ of the dipole transition moment with respect to the normal of the thin film stack. So the two orientations || and $\perp$ refer to a parallel (φ=90°) and perpendicular (φ=0°) emitter alignment, respectively.

Eq. (1) describes the emission pattern for an arbitrary orientation based on the emission patterns of the basic orthogonal dipoles in the stationary case. However, a correct quantitative description needs to consider the Purcell effect, i.e., modification of the emissive lifetime due to the optical cavity. An emitter with a limited internal quantum efficiency *Q* will exhibit the orientation dependent rate Γ, thus resulting in the emission pattern

$$I(\theta,\varphi,Q) = \frac{1}{\Gamma(Q,\varphi)} * I^{stat}(\theta,\varphi) \quad \text{with} \quad (2)$$

$$\Gamma(Q,\varphi) = \Gamma_{||}(Q)\sin^2(\varphi) + \Gamma_{\perp}(Q)\cos^2(\varphi) \quad . \quad (3)$$

Usually, the emission is due to an ensemble of incoherently emitting molecules. The ensemble average is observable experimentally and follows from eq. (1) or eq. (2) by including the orientation distribution *g(φ)* of the molecular ensemble. This yields the “parallel” and “perpendicular” emitter contributions

$$\left|p_{||}\right|^2 = \int g(\varphi)\sin^2\varphi\sin\varphi\, d\varphi \quad , \text{ and} \quad (4)$$

$$|p_{\perp}|^2 = \int g(\varphi)\, cos^2\varphi\sin\varphi\, d\varphi \quad . \quad (5)$$

With these second moments of the orientation distribution one obtains the stationary pattern and the ensemble emission rate from eq. (1) and (3) according to

$$\langle I^{stat}(\theta)\rangle_{\varphi} = |\mathrm{p}_{||}|^2 \cdot \left(I_{||,TE}(\theta) + I_{||,TM}(\theta)\right) + |\mathrm{p}_{\perp}|^2 \cdot I_{\perp,TM}(\theta) \quad (6)$$

$$\langle \Gamma(Q,\varphi)\rangle_{\varphi} = |\mathrm{p}_{||}|^2 \cdot \Gamma_{||}(Q) + |\mathrm{p}_{\perp}|^2 \cdot \Gamma_{\perp}(Q) \quad . \quad (7)$$

1.4 Limitations and target

With regard to section 1.2 above, the emission pattern as well as the lifetime method determine the ratio $|\mathrm{p}_{||}|^2 : |\mathrm{p}_{\perp}|^2$ of these parameters experimentally by exploiting the emission pattern from equation (1) or the excited state lifetime in equation (3). This corresponds to a measurement of the average orientation angle, which represents the emission pattern (or the emission lifetime) of the ensemble. Because only the ratio of the second moments of the orientation distribution according to eqs. (4) and (5) is obtained, the two distributions shown in Figure 1.1 cannot be distinguished from an isotropic emitter ensemble.

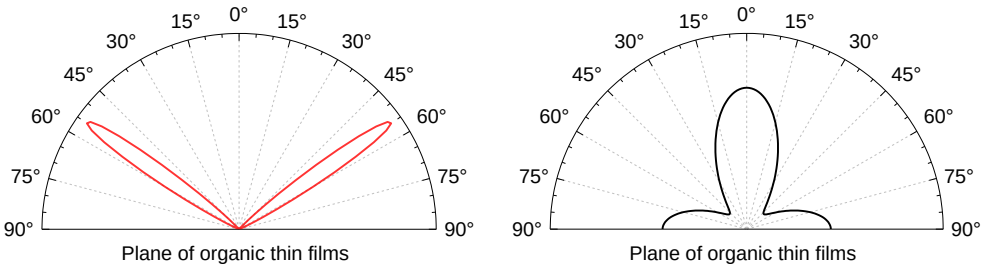

Figure 1.1: Sketch of two orientation distributions g(φ) which cannot be distinguished from the isotropic case corresponding to g(φ)=constant.

Therefore, the present approach intends to gain more knowledge about details of the orientation distribution of molecular emitting ensembles.

2 Experimental Set-up

2.1 Principle of operation

Recently, an approach exploiting both the pattern and the emission lifetime features has been suggested.[9] Following a short excitation, each emitter in the molecular ensemble will exhibit a single exponential decay with an emission rate according to its orientation. Then, the temporal decay will be of the form

$$\langle I(t,\theta,Q)\rangle_{\varphi} = \left\langle I^{stat}(\theta,\varphi)\cdot \mathrm{e}^{-\Gamma(\mathrm{Q},\varphi)\cdot \mathrm{t}}\right\rangle_{\varphi} \quad . \tag{8}$$

Whenever the emission rate Γ depends on the emitter orientation, this equation describes a non-exponential temporal evolution of the observed intensity. Such deviation from a mono-exponential decay will depend on two major facts:

- the orientation dependent splitting of the emission rates for parallel and perpendicular emitters, and
- different detection efficiencies for the different molecular orientations according to the observation angle.

These two issues will be discussed in detail below.

2.2 Sample design

2.2.1 Standard OLED

First, a standard bottom emitting OLED is considered. For the sake of simplicity the following considerations restrict on the monochrome case (λ = 550 nm) and a single organic material with refractive index n_{org}=1.75. The latter approximates the injection, transport, and emissive layers as well as ITO. The value of n_s=1.45 is used as (fused silica like) substrate refractive index and a metal cathode made of Aluminum is considered (n_{Al}=1.20+7.20i). In such simplified situation, the emission lifetimes of parallel and perpendicular emitters differ significantly close to the metal only. For a separation of approximately 20 nm between emitter and cathode, the perpendicular dipole transfers the major part of its energy into the surface plasmon polariton at the metal interface, thus increasing its decay rate and reducing its lifetime. For large emitter – cathode separations the lifetime ratio oscillates around the value of one. One does not expect significant non-exponential effects because of such small variations for large distances to the metal.

Figure 2.2 illustrates the transient observation inside the substrate expected for different cases of emitter orientation. A strictly aligned ensemble (i.e. parallel, perpendicular, or a narrow angular distribution) will exhibit a single exponential decay. The emission of a wide orientation distribution, which is shown for the isotropic ensemble, will emit a superposition of several exponential decays. The dashed blue curve in Figure 2.2 shows a fast decay at short times that is due to the short emission lifetime of perpendicular emitters. In contrast, the TE polarized observation detects mainly emission from parallel emitters. Therefore, deviation from a single exponential decay is small and the lifetime observed is close to the value of strictly parallel emitters.

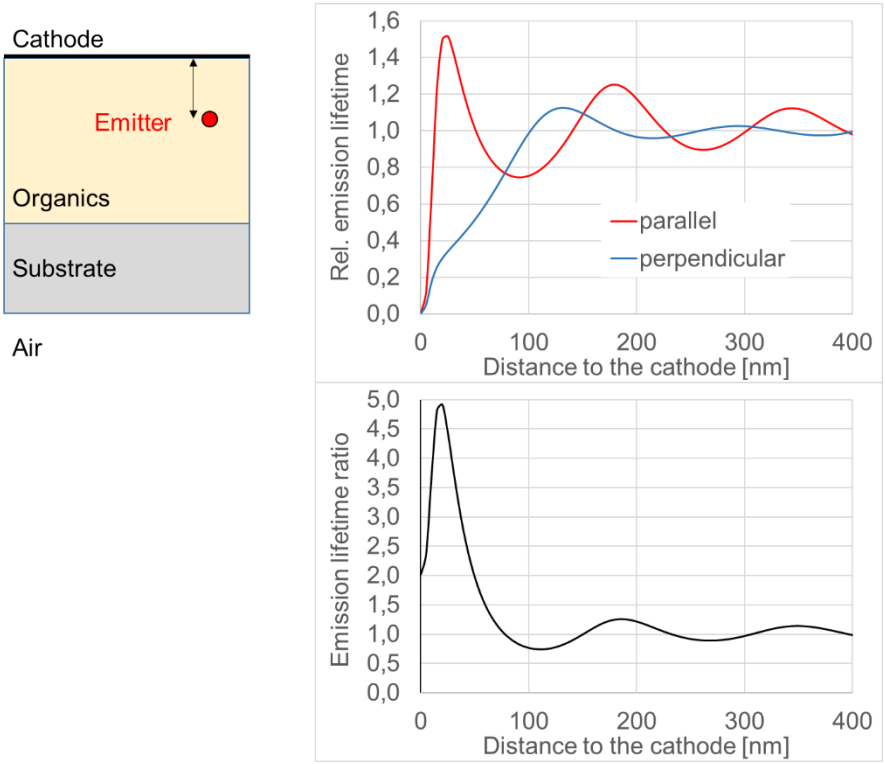

Figure 2.1: Sketch of the simplified OLED set-up (top left), the emission lifetimes of parallel and perpendicular emitters (top right), the ratio between these two lifetime curves (bottom left).

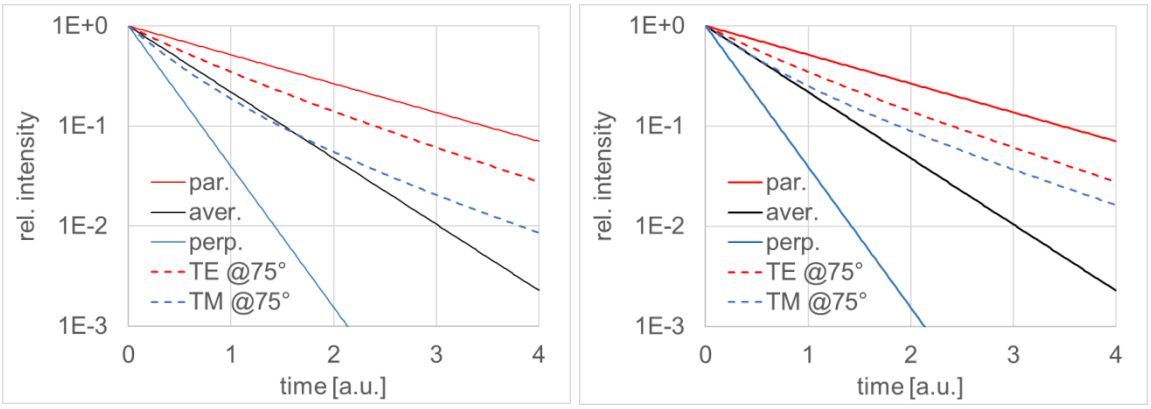

Figure 2.2: Transient intensities (normalized at t=0) in logarithmic scale for emitters separated 20 nm from the metal cathode (refer to Figure 2.1). The curves show strictly parallel (red) and perpendicular (blue) emitters exhibiting the extreme lifetimes, whilst the black curve illustrates a narrow angular distribution according to Figure 1.1 left. The two dashed curves illustrated the expected emission of an isotropic ensemble for two polarizations. The left diagram assumes observation in the substrate, the right one in air.

This effect is well apparent when analysing the temporal emission inside the substrate (Figure 2.2 left). If one observes the emission in air, the contribution of the perpendicular emitters to the emission pattern is rather low. Thus, the difference between the TE and TM polarized observations is reduced (Figure 2.2 right).

An isotropic ensemble is assumed for the present simulations, and this ensemble is expected to be excited without any preferred orientation, e.g. due to electrical pumping. The lifetime

effects can become more pronounced when pumping the luminescing ensemble optically, because emitters parallel aligned to the input polarization will be excited preferably.

Please note, that for observation angles zero, i.e. perpendicular observation, no effect between the two dashed curves can appear. This is because in such observation geometry the parallel components of the emitters are observed only.

From the considerations above one might suspect that the standard OLED stack's emission with reduced emitter-cathode-distance is an ideal configuration to deduce additional features of the dipole orientation distribution. However, it is not well suited for a standard orientation characterization based on emission pattern analysis. The following facts illustrate this: For decreasing emitter-cathode-distance the (TM polarized) emission of perpendicular emitters is preferred due to constructive interference conditions, whilst that of parallel emitters decreases due to destructive interference conditions. But, the strong excitation of the plasmon-polariton causes the far-field emission of perpendicular emitters to drop considerably. Therefore, the (TM polarized) emission of perpendicular emitters is well below that of parallel emitters. This complicates accurate orientation analysis, which in an ideal case would require similar intensities of parallel and perpendicular emitters.

2.2.2 Microcavity OLED

One option to

(a) observe the desired effect in air and to
(b) adjust the power emitted into TE and TM polarizations

is to combine an existing approach with this new experimental scheme. Following the design rules from Refs. 4 and 5 requires one to increase the emitter – cathode separation to a value, which maximizes the emission of perpendicular emitters into air. For the present simplified OLED system this corresponds to approximately 165 nm.

In order to achieve orientation dependent lifetime splitting, which usually disappears at such distances, an additional semi-transparent metal layer is introduced at the anode side of the OLED. Then, the ratio between parallel and perpendicular emission lifetimes can reach values in the range of four. This yields the transient emission illustrated in Figure 2.3, which compares to Figure 2.2 well.

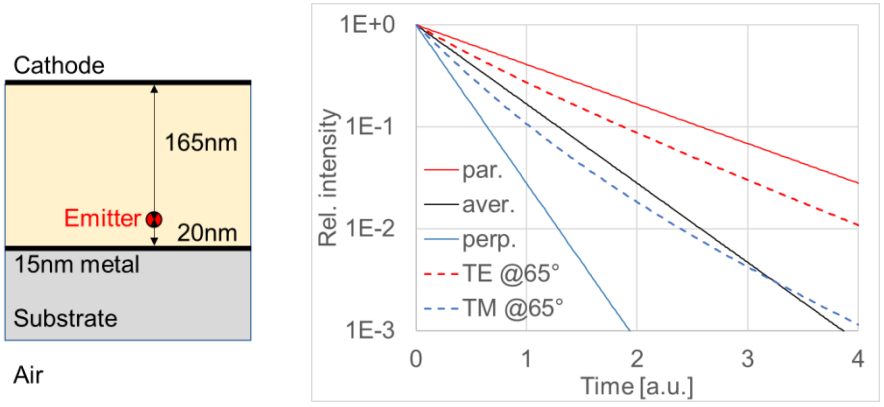

Figure 2.3: Sketch of the revised OLED system (left) as well as the transient behaviour expected in the experiment (dashed) with respect to strictly aligned emitters (solid). Colours are the same as in Figure 2.2.

So tuneable visibility of perpendicular emitters in the far field as well as tuneable orientation lifetime splitting (which is linked to the semi-transparent metal absorption) can be combined.

2.3 Experimental set-up design

2.3.1 Requirements

The experimental system for performing an orientation analysis based on eq. (8) needs to be set up. It has to perform the following tasks:

a. Transient emission lifetime analysis – In order to accurately measure the temporal evolution of fluorescence intensities. The emission lifetime ranges are expected to be in the nanosecond (fluorophores) to microsecond range (TADF or phosphors).
b. Optical excitation – In order to reach short emission lifetimes, a polarization controlled optical excitation in the picosecond temporal range is required. This can be used for exciting photoluminescence emission patterns.
c. Angularly resolved and polarization resolved detection – The emission needs to be observed under variable angles and polarizations in order to distinguish the signals originating from mainly parallel and perpendicular emitters.
d. Spectrally resolved analysis – Intends to perform standard orientation analysis with the same system. This shall ensure comparability of the data.

2.3.2 Sketch and Mechanical Design

Figure 2.4 sketches the intended optical set-up. The key approach is to keep both (i) the spectrally resolved as well as (ii) the temporally resolved detection fixed, whereas a goniometric rotation of the sample as well as of a picosecond laser diode is possible. This approach is chosen because (i) the transmission of multimode fibres depends on its bending which would introduce angle dependent effects, and (ii) the elevated weight of the single photon counting PMT.

As the set-up shall perform scans of the emission angle, the angular position of the excitation source can be fixed to the sample. This ensures constant excitation conditions during an experiment. The experimental approach is sketched Figure 2.4.

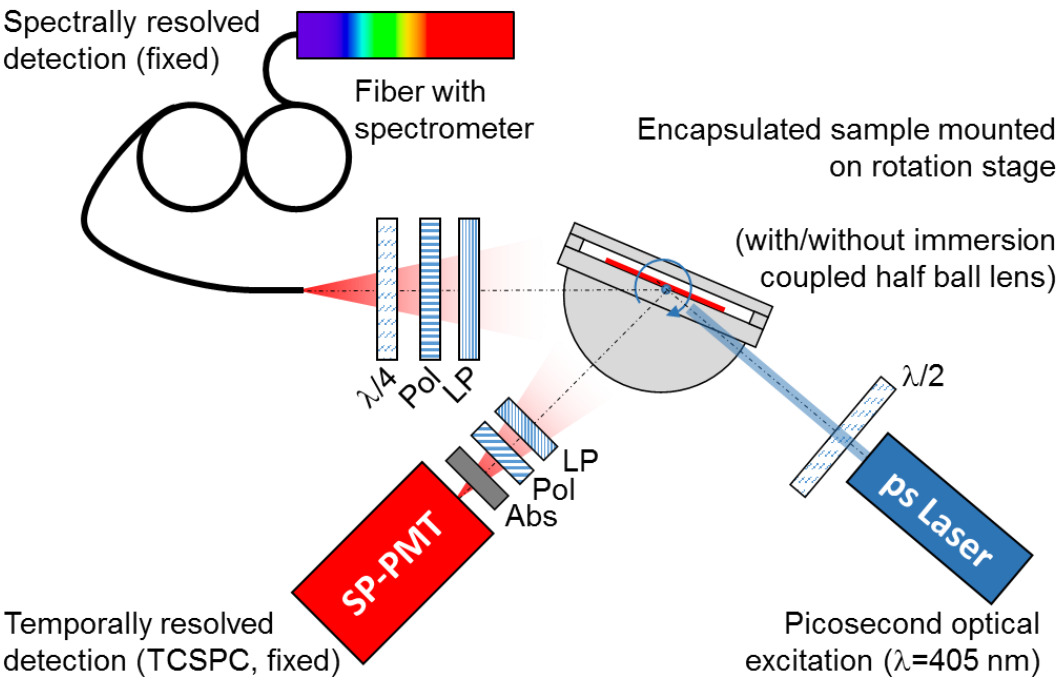

Figure 2.4: Schematic view of the set-up in order to analyse (encapsulated) organic thin film samples. Immersion coupling to a half ball lens should be possible to detect emission inside the substrate.

2.3.3 Description of key system components

Below, the key components of the system will be described:

Spectrally resolved analysis is based on a fibre spectrometer. A multimode fibre with NA 0.22, corresponding to ±12.7° acceptance angle, is the light collecting element. In order to avoid spectral or polarization effects inside the spectrometer, a mode mixer is used. Furthermore, a half wave plate ensures that – independent of the selected observation polarization – circularly polarized light is coupled into the fibre in order to avoid polarization dependent losses. For optical pumping, a long pass filter can be placed in front of this detection arm.

Temporal resolved analysis features a “Time Harp” (PicoQuant) single photon counting equipment that is capable of working in both nanosecond and micro second temporal ranges. The photon multiplier tube is equipped with a long pass filter for blocking excitation and a polarizer to select the observation polarization. Additional absorbing neutral density filters might reduce the count rate if necessary.

Optical excitation is achieved with a pulsed laser diode. The laser can be fixed mechanically with respect to the sample; its polarization can be adjusted by means of a quarter wave plate. This ensures that changing the polarization will not alter the illuminated position at the sample.

Alignment – The sample is mounted on an x,y,z mechanical stage in order to align the active area of the emitting surface with the rotation axis of the goniometer.

2.4 Final System

Figure 2.5 illustrates the final system with all elements sketched in Figure 2.4 mounted. In addition to the previous explanation, the detection arm is equipped with a fiber light source for alignment purposes.

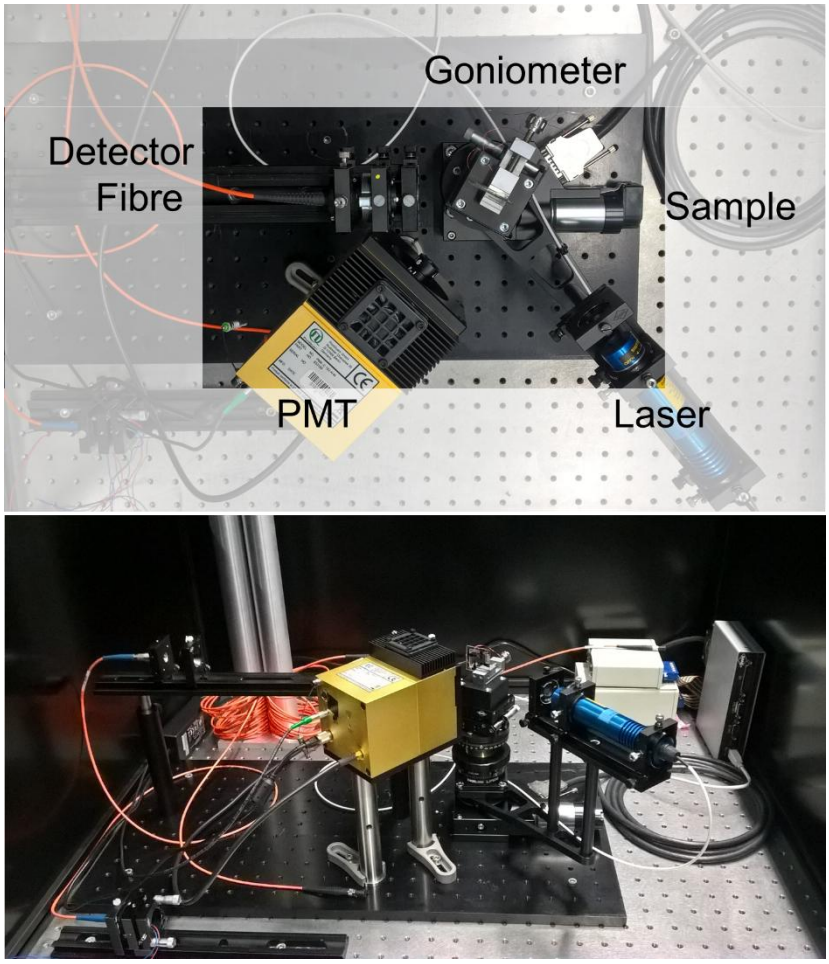

Figure 2.5: Photographs (top & side views) of the setup. The black housing is completely closed during operation to shield light from the surroundings.

For these settings, the PMT observation angle is aligned at 45° with respect to the spectral observation. Its angular acceptance range is given by the size of the photocatode (∅ 8 mm) and is in the range of approximately 5° full width.

The angular resolution of the spectrally resolved detection is determined by the size of the active area (~2 mm assumed) and the distance between fibre and sample. The present settings ensure an angular resolution below 2°.

The angular range for moving the illumination arm is -135° .. +99°, which is limited by the mechanical extension of the different elements.

2.5 Preliminary experimental results

Some examples for experimental data obtained with the set-up are shown below. Firstly, an emission pattern (along with simulation) for standard emitter characterization is shown in Figure 2.6. The destructive interference, which is exploited for emission zone analysis, is well visible in the TE polarized pattern. For TM, the contribution of perpendicularly aligned emitters at large angles is clearly visible.

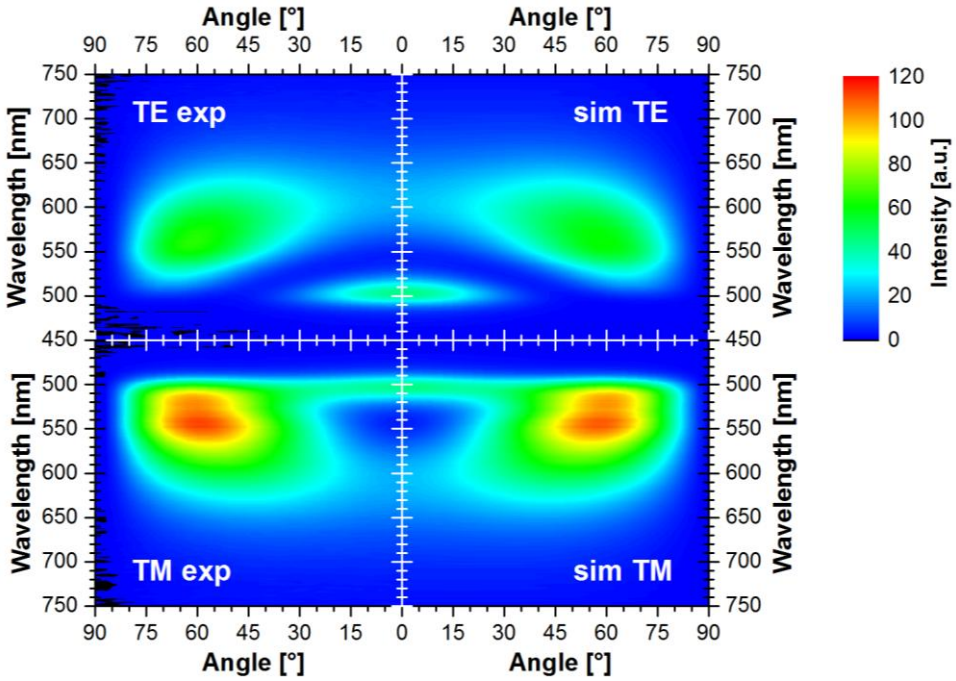

Figure 2.6: Angularly and spectrally resolved emission pattern observed in air for an Ir(ppy)$_3$ OLED in linear scale for two polarizations (left) shown with best fit (right) to derive emission zone and orientation. The OLED stack features an ETL thickness that yields destructive interference in TE polarization.

Electroluminescence time traces have been taken with electrical pumping for different OLEDs (Figure 2.7). Non-exponential decays are observed. Additionally, transient temporal traces have been taken for the OLED utilized in Figure 2.6 at different angles. The initial decay time is plotted for three observation angles and the two linear polarizations in Figure 2.8.

As expected, there is no significant variation of the decay time. This is due to two major effects: First, the emitter position features no significant orientation dependent lifetime splitting. Second, Ir(ppy)$_3$ has three ligands with degenerate transitions, so an “average” emission rate is observed for all observation conditions.

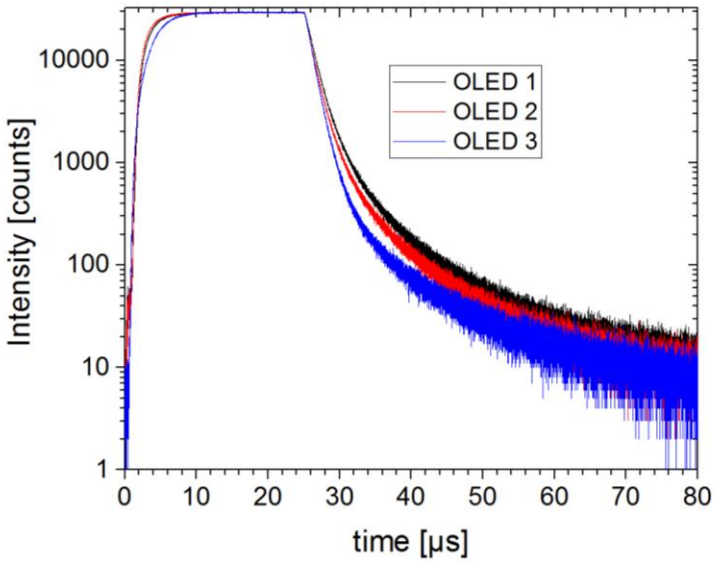

Figure 2.7: Transient time traces for 25 µs electrical pumping of three different OLED emitting materials.

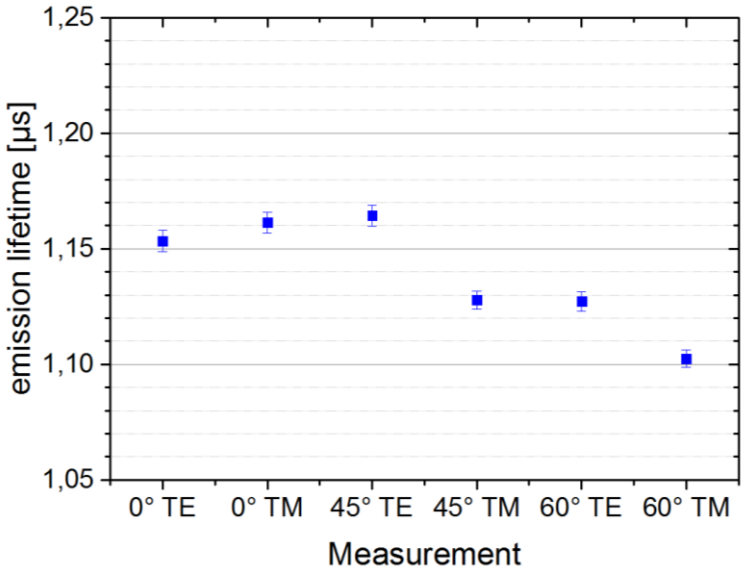

Figure 2.8: Initial decay times derived from the half ball lens coupled emission lifetimes for the $Ir(ppy)_3$ OLED stack from Figure 2.6.

3 Summary and Conclusions

3.1 Summary

The present task intends to extend the characterization capabilities for anisotropically aligned OLED emitters. Present approaches that rely on the quantitative analysis of polarized far-field patterns solely determine a single number as a measure of dipol orientation, e.g. the ratio $|p_{||}|^2:|p_{\perp}|^2$ of the second moments of the orientation distribution. This limitation prohibits one to distinguish qualitatively different orientation distribution functions. It shall be overcome by angularly resolved emission lifetime analyses of special samples.

The design of appropriate samples needs to consider two effects: Firstly, the emission of perpendicular emitters needs to be visible in the far-field. This requires uncommon ETL thicknesses as well known from emission pattern based determination of emission zone and orientation. Second, a large orientation dependent lifetime splitting needs to be reached by a thin metal layer in the vicinity of the emitters. Such a metal layer supports the propagation of surface plasmon polaritons, thus quenching the emission of perpendicular emitters while affecting parallel emitters to a lesser amount.

A set-up combining the classical, angularly and spectrally resolved analysis has been assembled with a time correlated single photon counting system. This enables to accurately observe the temporal luminescence evolution following a short electrical and/or optical pumping. Both, electrical and/or optical pumping can be used to detect lifetimes in the nanosecond … millisecond range.

3.2 Outlook

Currently, a study of stack designs is being prepared in order to derive optimized configurations for temporally resolving the width of the orientation distribution. Realistic emission spectra as well as birefringent materials in the organic thin film stack have to be taken into account for this analysis. The entire characterization capabilities will be applied to analyse those samples.

---

[1] Th. Förster, “Zwischenmolekulare Energiewanderung und Fluoreszenz,” Ann. Phys. 6, 55-75 (1948).

[2] J.-S. Kim, P. K. H. Ho, N. C. Greenham, and R. H. Friend, “Electroluminescence emission pattern of organic light-emitting diodes: Implications for device efficiency calculations,” J. Appl. Phys. 88, 1073-1081 (2000).

[3] S. H. Garret, J. A. E. Wasey, and W. L. Barnes, “Determining the orientation of the emissive dipole moment associated with dye molecules in microcavity structures,” J. Mod. Opt. 51(15), 2287–2295 (2004).

[4] M. Flämmich, M. C. Gather, N. Danz, D. Michaelis, A. H. Bräuer, K. Meerholz, and A. Tünnermann, “Orientation of emissive dipoles in OLEDs: Quantitative in situ analysis,” Org. Electron. 11, 1039-1046 (2010).

[5] M. Flämmich, D. Michaelis, N. Danz, “Accessing OLED emitter properties by radiation pattern analyses,” Org. Electron. 12, 83-91 (2011).

[6] J. Frischeisen, D. Yokoyama, C. Adachi, and W. Brütting, „Determination of molecular dipole orientation in doped fluorescent organic thin films by photoluminescence measurements,“ Appl. Phys. Lett. 96, 073302 (2010).

[7] T. D. Schmidt, D. S. Setz, M. Flämmich, J. Frischeisen, D. Michaelis, B. C. Krummacher, N. Danz, and Wolfgang Brütting, „Evidence for non-isotropic emitter orientation in a red phosphorescent organic light-emitting diode and its implications for determining the emitter’s radiative quantum efficiency,” Appl. Phys. Lett. 99, 163302 (2011).

[8] L. Penninck, F. Steinbacher, R. Krause, and K. Neyts, „Determining emissive dipole orientation in organic light emitting devices by decay time measurement,” Org. Electron. 13, 3079–3084 (2012).

[9] R. Mac Ciarnain, D. Michaelis, T. Wehlus, A. F. Rausch, S. Wehrmeister, T. D. Schmidt, W. Brütting, N. Danz, A. Bräuer, and A. Tünnermann, „Plasmonic Purcell effect reveals obliquely ordered phosphorescent emitters in Organic LEDs,“ Sci. Reports 7, 1826 (2017).